LPT–Orsay 07-135
SHEP-07-46
BONN-TH-2008-01
PTA/07-062

# Benchmark scenarios for the NMSSM

A. Djouadi[1,2,3], M. Drees[3], U. Ellwanger[1], R.Godbole[4], C. Hugonie[5], S.F. King[2], S. Lehti[6], S. Moretti[1,2], A. Nikitenko[7], I. Rottländer[3], M. Schumacher[8], A. M. Teixeira[1]

[1] Laboratoire de Physique Théorique, Université Paris–Sud, F–91405 Orsay Cedex, France.
[2] School of Physics and Astronomy, University of Southampton, Highfield, SO17 1BJ, UK.
[3] Physikalisches Institut, University of Bonn, Nussallee 12, 53115 Bonn, Germany.
[4] Center for High Energy Physics, Indian Institute of Science, Bangalore 560 012, India.
[5] LPTA, Université de Montpellier II, 34095 Montpellier, France.
[6] Helsinki Institute of Physics, P.O. Box 64, FIN-00014, University of Helsinki, Finland.
[7] Physics Department, Imperial College, Prince Consort Road, London SW7 2AZ, UK (on leave of absence from ITEP, Moscow, Russia).
[8] Fachbereich Physik, University of Siegen, Walter Flex Str. 3, 57068 Siegen, Germany.

**Abstract**

We discuss constrained and semi–constrained versions of the next–to–minimal supersymmetric extension of the Standard Model (NMSSM) in which a singlet Higgs superfield is added to the two doublet superfields that are present in the minimal extension (MSSM). This leads to a richer Higgs and neutralino spectrum and allows for many interesting phenomena that are not present in the MSSM. In particular, light Higgs particles are still allowed by current constraints and could appear as decay products of the heavier Higgs states, rendering their search rather difficult at the LHC. We propose benchmark scenarios which address the new phenomenological features, consistent with present constraints from colliders and with the dark matter relic density, and with (semi–)universal soft terms at the GUT scale. We present the corresponding spectra for the Higgs particles, their couplings to gauge bosons and fermions and their most important decay branching ratios. A brief survey of the search strategies for these states at the LHC is given.

## 1. Introduction

The next-to-minimal supersymmetric extension of the standard model (NMSSM), in which the spectrum of the minimal supersymmetric extension (MSSM) is extended by one singlet superfield, has been discussed since the early days of supersymmetry (SUSY) model–building [1–3]. In the last decade, the NMSSM gained a renewed interest in view of its positive features as compared to the widely studied MSSM. Firstly, the NMSSM naturally solves in an elegant way the so–called $\mu$ problem [4] of the MSSM: to have an acceptable phenomenology, a value in the vicinity of the electroweak or SUSY breaking scale is needed for the supersymmetric Higgs mass parameter $\mu$; this is automatically achieved in the NMSSM, since the $\mu$-parameter is dynamically generated when the singlet Higgs field acquires a vacuum expectation value of the order of the SUSY breaking scale, leading to a fundamentalLagrangian that contains no dimensionful parameters apart from the soft SUSY breaking terms. Secondly, as compared to the MSSM, the NMSSM can induce a richer phenomenology in the Higgs and neutralino sectors, both in collider and dark matter (DM) experiments: on the one hand, heavier Higgs states can decay into lighter ones with sizable rates [5–16] and, on the other hand, a new possibility appears for achieving the correct cosmological relic density [17] through the so-called "singlino", i.e. the fifth neutralino of the model, which can have weaker-than-usual couplings to standard model (SM) particles. Thirdly, the NMSSM needs somewhat less fine tuning [8, 18] (although some fine tuning is still required [19]): the upper limit on the mass of the lightest CP–even Higgs particle is larger than in the MSSM, and therefore more SUSY parameter space survives the bounds imposed by the negative Higgs boson searches at LEP; furthermore, possible unconventional decays of the SM–like Higgs scalar allow it to have a relatively small mass, well below the SM Higgs mass limit of 114 GeV, still consistent with LEP constraints.

Given the possibly quite different phenomenology in the Higgs sector as compared to the SM and the MSSM [20], it is important to address the question whether such NMSSM specific scenarios will be probed at the LHC. In particular, it would be important to extend the so-called "no-lose theorem" of the MSSM [21], which states that at least one MSSM Higgs particle should be observed at the LHC for the planned integrated luminosity, to the NMSSM [6, 22] or try to define regions of the NMSSM parameter space where more Higgs states are visible at the LHC than those available within the MSSM [23]. However, a potential drawback of the NMSSM, at least in its non constrained versions, is that it leads to a larger number of input parameters in the Higgs sector to deal with, compared to the MSSM. In particular, it is clearly unfeasible to perform multi-dimensional "continuous" scans over the free inputs of the NMSSM, especially if each sampled point is subject to a complete simulation in order to be as close as possible to the experimental conditions.

An alternative approach, acknowledged by both the theoretical and experimental communities, is that of resorting to the definition of so-called "benchmark points" (or slopes, or surfaces) in the SUSY parameter space [24]. These consist of a few "discrete" parame-

ter configurations of a given SUSY model, which embody the most peculiar/representative phenomenological features of the model's parameter space. Using discrete points avoids scanning the entire parameter space, focusing instead on representative choices that reflect the new interesting features of the model, such as new signals, peculiar mass spectra, etc. A reduced number of points can then be subject to full experimental investigation, without loss of substantial theoretical information.

While several such benchmark scenarios have been devised for the MSSM [24, 25] and thoroughly studied in both the collider and the DM contexts, limited progress has been made so far in this direction for the case of the NMSSM. In Ref. [9], an earlier attempt was made to address the possibility of establishing a no-lose theorem for the NMSSM Higgs sector at the LHC through benchmark points (in a non-universal low energy setup in which the SUSY particles are very heavy). However, the corresponding spectrum was not consistent with DM constraints (in particular on the lightest SUSY particle, LSP), which were not yet established for the NMSSM at the time. In addition, many of the points discussed in Ref. [9] have become ruled out due to the new lower value of the top quark mass, and to more stringent constraints from collider searches and precision measurements. Also the tools to calculate the Higgs and SUSY particle spectra have been upgraded since then [26, 27].

In this report, we build on the experience of Ref. [9] and define benchmark points which fulfill the present collider and cosmological constraints using the most up-to-date tools to calculate the particle spectra. However, in contrast to Ref. [9], we work in the framework of a (semi–)constrained NMSSM parameter space, henceforth called cNMSSM, where the soft SUSY–breaking parameters are defined at the Grand Unified (GUT) scale: on the one hand, this approach leads to a much more plausible sparticle spectrum and allows one to relate features of the Higgs sector to properties of the neutralino sector (and hence of the LSP); on the other hand, this restricted parameter space still contains the phenomenological features of the NMSSM that are very distinctive from those of the MSSM, and is suitable for intensive phenomenological investigation by the experimental collaborations. The emphasis will primarily be on the different possible scenarios within the Higgs sector and the implication for Higgs searches at the LHC. However, we will also comment on the possible implications of these benchmark points for the cosmological relic density of the lightest neutralino DM candidate. Finally, we will describe the tools used to define such benchmark scenarios.

The report is organized as follows. In the next section, we define the NMSSM and its particle content with some emphasis on constrained scenarios defined in terms of soft terms specified at the GUT scale, discuss the tools that allow to calculate the particle spectrum, and the various constraints that should be imposed on the latter. In section 3, we propose five benchmark points which lead to Higgs sectors that are different from those of the MSSM and discuss their main features. In section 4, we outline the possible search strategies at the LHC for the Higgs particles in these scenarios. A brief outlook is given in section 5.

## 2. The NMSSM and its particle spectrum

### 2.1 The unconstrained NMSSM

In this paper, we confine ourselves to the NMSSM with a scale invariant superpotential. Alternative generalizations of the MSSM – known as the minimal non-minimal supersymmetric SM (MNSSM), new minimally-extended supersymmetric SM or nearly-minimal supersymmetric SM (nMSSM) or with additional U(1)' gauge symmetries – exist [28], but these will not be considered here, nor the case of explicit CP violation [29]. The scale invariant superpotential of the NMSSM is given, in terms of (hatted) superfields, by

$$\mathcal{W} = \lambda \widehat{S}\widehat{H}_u\widehat{H}_d + \frac{\kappa}{3}\,\widehat{S}^3 + h_t\widehat{Q}\widehat{H}_u\widehat{t}^c_R - h_b\widehat{Q}\widehat{H}_d\widehat{b}^c_R - h_\tau\widehat{L}\widehat{H}_d\widehat{\tau}^c_R \tag{1}$$

in which only the third generation fermions have been included (with possible neutrino Yukawa couplings have been set to zero), and $\widehat{Q}, \widehat{L}$ stand for superfields associated with the $(t, b)$ and $(\tau, \nu_\tau)$ SU(2) doublets. The first two terms substitute the $\mu\widehat{H}_u\widehat{H}_d$ term in the MSSM superpotential, while the three last terms are the usual generalization of the Yukawa interactions. The soft SUSY breaking terms consist of the scalar mass terms for the Higgs and sfermion scalar fields which, in terms of the fields corresponding to the complex scalar components of the superfields, are given by

$$\begin{aligned} -\mathcal{L}_{\rm mass} &= m^2_{H_u}|H_u|^2 + m^2_{H_d}|H_d|^2 + m^2_S|S|^2 \\ &+ m^2_{\tilde{Q}}|\tilde{Q}^2| + m^2_{\tilde{t}_R}|\tilde{t}^2_R| + m^2_{\tilde{b}_R}|\tilde{b}^2_R| + m^2_{\tilde{L}}|\tilde{L}^2| + m^2_{\tilde{\tau}_R}|\tilde{\tau}^2_R| \,, \end{aligned} \tag{2}$$

and the trilinear interactions between the sfermion and Higgs fields,

$$-\mathcal{L}_{\rm tril} = \lambda A_\lambda H_u H_d S + \frac{1}{3}\kappa A_\kappa S^3 + h_t A_t \tilde{Q} H_u \tilde{t}^c_R - h_b A_b \tilde{Q} H_d \tilde{b}^c_R - h_\tau A_\tau \tilde{L} H_d \tilde{\tau}^c_R + \text{h.c.}\,. \tag{3}$$

In an unconstrained NMSSM with non–universal soft terms at the GUT scale, the three SUSY breaking masses squared for $H_u$, $H_d$ and $S$ appearing in $\mathcal{L}_{\rm mass}$ can be expressed in terms of their vevs through the three minimization conditions of the scalar potential. Thus, in contrast to the MSSM (where one has only two free parameters at the tree level, generally chosen to be the ratio of Higgs vacuum expectation values (vevs) $\tan\beta$ and the mass of the pseudoscalar Higgs boson), the Higgs sector of the NMSSM is described by the six parameters

$$\lambda \ , \ \kappa \ , \ A_\lambda \ , \ A_\kappa, \ \tan\beta = \ \langle H_u\rangle/\langle H_d\rangle \text{ and } \mu_{\rm eff} = \lambda\langle S\rangle \ . \tag{4}$$

One can choose sign conventions such that the parameters $\lambda$ and $\tan\beta$ are positive, while the parameters $\kappa$, $A_\lambda$, $A_\kappa$ and $\mu_{\rm eff}$ can have both signs.

In addition to the above parameters of the Higgs sector, one needs to specify the soft SUSY breaking mass terms in eq. (2) for the scalars, the trilinear couplings in eq. (3) as well as the gaugino soft SUSY breaking mass parameters to describe the model completely,

$$-\mathcal{L}_{\rm gauginos} = \frac{1}{2}\Big[M_1\tilde{B}\tilde{B} + M_2\sum_{a=1}^{3}\tilde{W}^a\tilde{W}_a + M_3\sum_{a=1}^{8}\tilde{G}^a\tilde{G}_a \ + \ \text{h.c.}\Big]. \tag{5}$$

Clearly, in the limit $\lambda \to 0$ with finite $\mu_{\rm eff}$, the NMSSM turns into the MSSM with a decoupled singlet sector. Whereas the phenomenology of the NMSSM for $\lambda \to 0$ could still differ somewhat from the MSSM in the case where the lightest SUSY particle is the singlino (and hence with the possibility of a long lived next-to-lightest SUSY particle [30]), we will not consider this situation here.

### 2.2 The constrained NMSSM

As the number of input parameters is rather large, one can attempt to define a constrained model, hereafter called the cNMSSM, in which the soft SUSY–breaking parameters are fixed at the GUT scale, leading to only a handful of free input parameters to cope with. This approach is motivated by the fact that in many schemes for SUSY–breaking, the soft SUSY breaking parameters are predicted to be universal at a very high energy scale. For example, in the cMSSM or mSUGRA scenario, one imposes a common gaugino mass $M_{1/2}$, a scalar mass $m_0$ and a trilinear coupling $A_0$ at $M_{\rm GUT}$, leading to only four continuous free parameters (together with $\tan\beta$) and the sign of $\mu$. The values of the numerous soft SUSY–breaking parameters at low energies are then obtained through the renormalization group evolution (RGE). Analogously, the cNMSSM allows to describe the entire sparticle spectrum, including the chargino and neutralino sectors, in terms of a small number of free parameters. This is in contrast to the usual procedure where one postulates universal sfermion masses directly at the weak scale which seems less plausible since these masses would then be non–universal at the high (GUT) scale.

In analogy to the cMSSM, one can impose unification of the soft SUSY–breaking gaugino masses, sfermion and Higgs masses and trilinear couplings at the scale $M_{\rm GUT}$:

$$M_{1,2,3} \equiv M_{1/2} \ , \quad m_{\tilde{F}_i} = m_{H_i} \equiv m_0 \ , \quad A_i \equiv A_0 \ . \tag{6}$$

The cMSSM has two additional parameters ($\mu$ and $B$) beyond those in eq. (6), but the correct value of $M_{Z^0}$ imposes one constraint (typically used to determine $|\mu|$) and $B$ can be replaced by $\tan\beta$. Likewise, the fully constrained NMSSM has two additional parameters ($\lambda$ and $\kappa$) beyond the three parameters in eq. (6), and the correct value of $M_{Z^0}$ imposes one constraint. Hence, a priori the number of free parameters in the cMSSM and the fully constrained NMSSM is the same.

In principle, one could minimize the effective potential of the cNMSSM with respect to $H_u$, $H_d$ and $S$, and determine the overall scale of the soft terms in eq. (6) from the correct value of $M_{Z^0}$: this approach has been pursued in Ref. [2]. However, since $\tan\beta$ is then obtained as output (while the top quark Yukawa coupling $h_t$ is an input), it becomes very difficult to obtain the correct value for $m_{\rm top}$. Also, the numerical minimization of the effective potential including radiative corrections is quite computer-time consuming.

Therefore it is much more convenient to employ the analytic form of the three minimization conditions of the effective potential of the NMSSM: for given $M_{Z^0}$, $\tan\beta$, $\lambda$ and

all soft terms at the weak scale (except for $m_S^2$), these can be solved for $|\mu_{\rm eff}|$ (or $|\langle S\rangle|$), $\kappa$ and $m_S^2$. As in the cMSSM, the sign of $\mu_{\rm eff}$ can still be chosen at will; in some sense, the determination of the parameter $B$ through the minimization conditions of the MSSM is replaced by the determination of $\kappa$ in the NMSSM and the additional minimization w.r.t. $\langle S\rangle$ in the NMSSM leads to the determination of $m_S^2$.

Assuming the weak scale soft scalar masses (apart from $m_S^2$) to arise from a unified scalar mass $m_0^2$, the determined weak scale value of $m_S^2$ – when run up to the GUT scale – will not coincide with $m_0^2$ in general. One could confine oneself to regions in parameter space where the difference between $m_S^2$ and $m_0^2$ is negligibly small, but we found that the phenomenology of this fully constrained NMSSM hardly differs (at least in the Higgs sector on which we are focusing here) from the one of the cMSSM once present LEP constraints are imposed. Hence we will relax the hypothesis of complete unification of the soft terms in the singlet sector since the singlet could play a special rôle[1], and we will allow for both $m_S^2 \neq m_0^2$ and $A_\kappa \neq A_0$ at $M_{\rm GUT}$. Note that, although $m_S^2$ at $M_{\rm GUT}$ can be negative, this does *not* signal an instability of the potential: the direction $\langle S\rangle \to \infty$ is always protected by a quartic self coupling $\sim \kappa^2$, which leads to $\langle S\rangle \sim M_{\rm SUSY}$ at the minimum of the potential.

In addition, for some of the benchmark points (see points P4 and P5 below), we will also relax the unification hypothesis for $m_{H_u}^2$ and $m_{H_d}^2$, in analogy to corresponding scenarios within the MSSM (called non-universal Higgs model or NUHM [32]). The hypothesis $A_\lambda = A_0$ will also be relaxed for point 5. Such points in parameter space can have additional unconventional properties, whose phenomenology should also be investigated.

### 2.3 The Higgs and SUSY spectra

Following the procedure employed by the routine NMSPEC within NMSSMTools [27], which calculates the spectra of the Higgs and SUSY particles in the NMSSM, a point in the parameter space of the cNMSSM is defined by the soft SUSY breaking terms at $M_{\rm GUT}$ (except for the parameter $m_S^2$), $\tan\beta$ at the weak scale, $\lambda$ at the SUSY scale (defined as an average of the first generation squark masses) and the sign of the parameter $\mu_{\rm eff}$. The parameters $\kappa$, $m_S^2$ and $|\mu_{\rm eff}|$ are determined at the SUSY scale in terms of the other parameters through the minimization equations of the scalar potential.

The RGEs for the gauge and Yukawa couplings have to be integrated from the weak scale up to $M_{\rm GUT}$ (defined by the unification of the gauge couplings $g_1$ and $g_2$), and the RGEs for the soft terms from $M_{\rm GUT}$ down to the weak scale. Since $\kappa$ and $m_S^2$ are computed at the weak scale, and threshold effects for the gauge and Yukawa couplings depend on the soft terms at the SUSY scale, some iterations are necessary in order to satisfy the desired boundary conditions for the soft terms at the GUT scale, but usually the procedure converges quite rapidly (at least for not too large values of $\tan\beta$ or $\lambda$). For the most

[1] An example is when the singlet is mixed with or identified with a radion originating from a 5d brane world [31]; however, here we do not consider a Kaluza-Klein mass scale below $M_{\rm GUT}$.

relevant SM parameters, the strong coupling and the top/bottom quark masses, we chose $\alpha_s(M_{Z^0}) = 0.1172$, $m_b(m_b)^{\overline{\rm MS}} = 4.214$ GeV and $m_{\rm top}^{\rm pole} = 171.4$ GeV.

After RGE running is completed, the gluino, chargino, neutralino and sfermion masses are computed including dominant one loop corrections to their pole masses. The lightest scalar Higgs pole mass is determined to the following accuracy (in a notation where its tree level mass is proportional to $\mathcal{O}(g^2)$, where $g$ denotes any of the electroweak gauge couplings): one loop corrections of $\mathcal{O}(h_{t,b}^4)$ and $\mathcal{O}(h_{t,b}^2\, g^2)$ are computed exactly; one loop corrections of the orders $g^4$, $g^2\lambda^2$, $\lambda^4$, $g^2\kappa^2$, $\kappa^4$ and $\lambda^2\kappa^2$ include only terms involving large logarithms $\ln(M_i^2/M_{Z^0}^2)$, where $M_i$ are potentially large Higgs or sparticle masses, while two loop corrections of $\mathcal{O}(h_{t,b}^6)$ and $\mathcal{O}(h_{t,b}^4\alpha_s)$ include only terms with two powers of large logs.

Once the pole masses are known, all Higgs decay branching ratios into SM and SUSY particles (an adaptation of the decays in the MSSM [33] to the NMSSM case) are determined including dominant (mainly QCD) radiative corrections [34], as well as sparticle loops which contribute to the couplings of a neutral Higgs to two photons or gluons [35].

When the spectrum and the couplings of the Higgs and SUSY particles are computed, available Tevatron and LEP constraints are checked. The results of the four LEP collaborations, combined by the LEP Higgs working group, are included [36]. More specifically, the following experimental constraints are taken into account:

(i) The masses of the neutralino as well as their couplings to the $Z^0$ boson are compared with the LEP constraints from direct searches and from the invisible $Z^0$ boson width;

(ii) Direct bounds from LEP and Tevatron on the masses of the charged particles ($h^\pm$, $\chi^\pm$, $\tilde{q}$, $\tilde{l}$) and the gluino are taken into account;

(iii) Constraints on the Higgs production rates from all channels studied at LEP. These include in particular $Z^0 h_i^0$ production, $h_i^0$ being any of the CP–even Higgs particles, with all possible two body decay modes of $h_i^0$ (into $b$ quarks, $\tau$ leptons, jets, photons or invisible), and all possible decay modes of $h_i^0$ of the form $h_i^0 \to a_j^0 a_j^0$, $a_j^0$ being any of the CP–odd Higgs particles, with all possible combinations of $a_j^0$ decays into $b$ quarks, $c$ quarks, $\tau$ leptons and jets. Also considered is the associated production mode $e^+e^- \to h_i^0 a_j^0$ with, possibly, $h_i^0 \to a_j^0 a_j^0$. (In practice, for our purposes, only combinations of $i = 1, 2$ with $j = 1$ are phenomenologically relevant.)

We stress that light Higgs scalars (with $M_{h_{1,2}^0} \lesssim 114$ GeV) can still be allowed by LEP constraints, if either (i) the $Z^0$–$Z^0$-$h_{1,2}^0$ coupling is heavily suppressed (if, for instance, the state $h_i^0$ is dominantly a gauge singlet); or (ii) $M_{a_1^0} \lesssim 11\,\text{GeV}$ such that the state $h_{1,2}^0$ decays dominantly into $a_1^0 a_1^0$ states, but the $b\bar{b}$ decay of $a_1^0$ is impossible; constraints from the decays $h_{1,2}^0 \to a_1^0 a_1^0 \to 4\tau$ allow for $M_{h_{1,2}^0}$ down to $\sim 86$ GeV. It is important to note, however, that LEP constraints are implemented only for individual processes, and that combinations of different processes could potentially rule out seemingly viable scenarios.

Finally, experimental constraints from B physics [37] such as the branching ratios of the rare decays $\text{BR}(B \to X_s\gamma)$, $\text{BR}(B_s \to \mu^+\mu^-)$ and $\text{BR}(B^+ \to \tau^+\nu_\tau)$ and the mass differences

$\Delta M_s$ and $\Delta M_d$, are also implemented; compatibility of each point in parameter space with the current experimental bounds is required at the two sigma level.

The new features of the NMSSM have an impact on the properties of the lightest neutralino as a dark matter candidate [17]. For instance, given the presence of a fifth neutralino (singlino), the composition of the annihilating WIMPs can be significantly different from those within the MSSM in wide regions of the parameter space. In particular, the LSP can have a large singlino component, in which case one has new couplings of the LSP to singlet-like Higgs states whose mass can be substantially lighter than the Higgs states within the MSSM. In the presence of light $h_1^0$ and $a_1^0$ states, there are new channels through which neutralino annihilation can occur in the NMSSM: $Z^0\, h_1^0$, $h_1^0\, h_1^0$, $h_1^0\, a_1^0$ and $a_1^0\, a_1^0$, either via $s$–channel $Z^0$, $a_i^0$, $h_i^0$ or $t$–channel neutralino exchange [17]. Among the proposed benchmark points, we will find examples of these new features.

Technically, the relic abundance of the NMSSM dark matter candidate $\chi_1^0$ is evaluated via a link to MicrOMEGAS [38]. All the relevant cross sections for the lightest neutralino annihilation and co-annihilation are computed. The density evolution equation is numerically solved and the relic density of $\chi_1^0$ is calculated. The result is compared with the "WMAP" constraint $0.094 \lesssim \Omega_{\rm CDM} h^2 \lesssim 0.136$ at the $2\sigma$ level [39].

## 3. The benchmark points

As already mentioned in the introduction, in view of the upcoming LHC, quite some work has been dedicated to probe the NMSSM Higgs sector over the recent years. In the NMSSM, two different types of scenarios have been pointed out, depending on whether Higgs-to-Higgs decays are kinematically allowed or forbidden. Within the first category, where Higgs-to-Higgs decays are kinematically allowed and can be dominant, there are two possibilities, each associated with light scalar/pseudoscalar Higgs states:

(i) The lightest pseudoscalar Higgs boson $a_1^0$ is rather light, $M_{a_1^0} \lesssim$ 40–50 GeV, and the lightest CP–even Higgs particle $h_1^0$ has enough phase space for the decay into two pseudoscalar Higgs particles, $h_1^0 \to a_1^0 a_1^0$, to be kinematically accessible. In this case, the branching ratio for the decay $h_1^0 \to a_1^0 a_1^0$ is typically very large and this new decay channel is the dominant one. Concerning the lightest pseudoscalar decays, there are two further possibilities: either $M_{a_1^0} \gtrsim 10$ GeV and the $a_1^0$ boson decays into a pair of $b$ quarks or a pair of tau leptons (with the former decay being in general dominant), leading to $h_1^0 \to a_1^0 a_1^0 \to 4\tau, 4b$ and $2\tau 2b$ final states, or $M_{a_1^0} \lesssim 10$ GeV and the dominant decay mode of the $a_1^0$ boson is into a pair of tau leptons, leading to $h_1^0 \to a_1^0 a_1^0 \to 4\tau$ final states. In this latter scenario, one can still distinguish two situations for the $h_1^0$ boson: its mass is either close to its theoretical upper limit of 130 GeV (within the cNMSSM), or to the lower limit of 90 GeV, still in agreement with constraints from Higgs boson searches at LEP2.

(ii) The lightest CP–even Higgs boson is relatively light, $M_{h_1^0} \lesssim 50$ GeV, and decays into $b\bar{b}$ pairs. (The situation where $M_{h_1^0} \lesssim 10$ GeV, such that the latter channel is kinematically

closed and the decay $h_1^0 \to \tau^+\tau^-$ dominates, is very constrained by LEP data.) In this case, the next-to-lightest CP even Higgs boson $h_2^0$ is SM–like, and has a mass below $\sim 150$ GeV. Even so, it can still decay into two $h_1^0$ bosons leading to the final topologies $h_2^0 \to h_1^0 h_1^0 \to 4\tau$, $2\tau 2b$ and $4b$, the latter final state being largely dominating.

The second category of scenarios, where Higgs-to-Higgs decays are suppressed, includes regions of the parameter space where all Higgs particles are relatively light with masses in the range 90–200 GeV. This opens the possibility of producing all the five neutral and the charged Higgs bosons at the LHC. This scenario is similar to the so–called "intense coupling regime" of the MSSM [40,41] (which has been shown to be rather difficult to be fully covered at the LHC), but with two more neutral Higgs particles.

In the context of the general NMSSM (without unification constraints), there exists also a decoupling regime in which all the Higgs bosons are heavy and decouple from the spectrum except for one CP–even Higgs particle, whose mass can be up to $\sim 140$ GeV [42]. Such decoupling scenarios are difficult to realize within the cNMSSM and, in any case, they would be very difficult to disentangle from an MSSM "$M_h^{\rm max}$"-scenario at the LHC, since the separation of the two would require a determination of the parameter $\tan\beta$ which is notoriously difficult to achieve at the LHC.

In the following, we propose five benchmark points of the NMSSM parameter space, P1 to P5, in which the above discussed scenarios are realized. Each point is representative of distinctive NMSSM features: points P1 to P3 exemplify scenarios where $h_1^0$ decays into light pseudoscalar states (decaying, in turn, into $b\bar{b}$ or $\tau^+\tau^-$ final states), P4 illustrates the NMSSM possibility of a very light $h_1^0$, while P5 corresponds to the case where all Higgs bosons are rather light. In all cases, the input parameters as well as the resulting Higgs masses and the relevant decay information are given in Table 1. In the subsequent Table 2, we summarize the most relevant features of each point regarding the cosmological relic density.

As discussed in Ref. [27], the scenarios where the pseudoscalar Higgs boson is light and the decay $h_1^0 \to a_1^0 a_1^0$ is dominant, can be realized within the cNMSSM with nearly universal soft terms at the GUT scale, the exception being the parameters $m_S^2$ and $A_\kappa$, which are chosen independently. A corresponding region in parameter space, containing P1, P2 and P3, is shown in Fig. 1, where we chose $m_0 = 174$ GeV, $M_{1/2} = 500$ GeV, $A_0 = -1500$ GeV, $\tan\beta = 10$ and the sign of $\mu_{\rm eff}$ is positive. As a function of the parameter $\lambda$, we show the values of $A_\kappa$ that are allowed by LEP constraints, the masses of the $h_1^0$ and $a_1^0$ bosons (where larger values of $M_{a_1^0}$ correspond to larger values of the trilinear coupling $|A_\kappa|$), and the dark matter relic density $\Omega_{\rm CDM}h^2$. The benchmark points P1, P2 and P3 discussed below are chosen at the upper and lower boundaries of this region of the cNMSSM parameter space. The lower limit on the pseudoscalar $a_1^0$ mass, $M_{a_1^0} \gtrsim 8$ GeV, in the last plot of Fig. 1 originates from constraints from B physics; see Ref. [37] for details.

In Fig. 2, we show the obtained results from a scan in the $[\lambda, A_\kappa]$ parameter space (with the values of the other parameters fixed to those used in Fig. 1) for the masses of the CP–

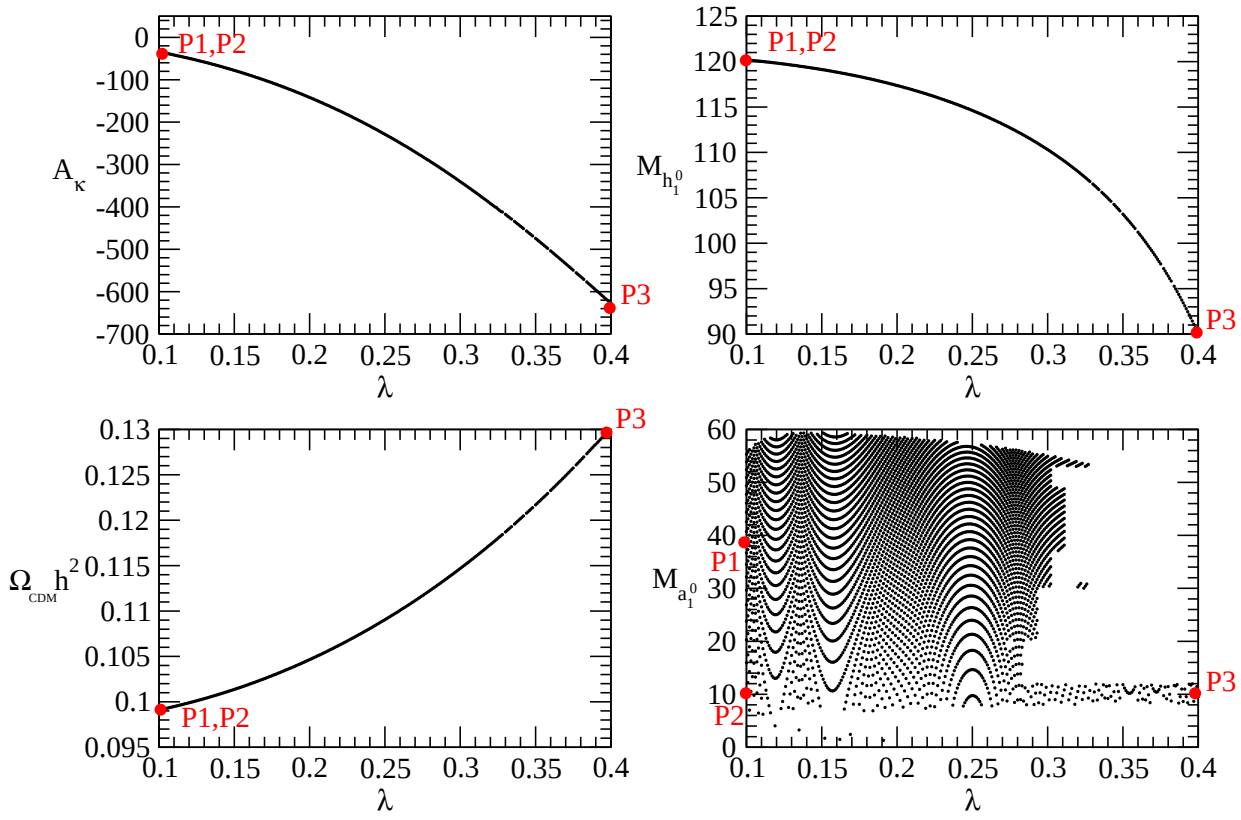


Figure 1: Allowed values of $A_\kappa$, $M_{h_1^0}$ and $M_{a_1^0}$ (in GeV) as well as $\Omega_{\rm CDM}h^2$ as a function of $\lambda$. We take $m_0 = 174$ GeV, $M_{1/2} = 500$ GeV, $A_0 = -1500$ GeV and $\tan\beta = 10$; $m_S^2$ is determined from the electroweak symmetry breaking conditions.

even $h_1^0$ and CP–odd $a_1^0$ states, as well as of the branching ratios of the decays $h_1^0 \to a_1^0 a_1^0$ and $a_1^0 \to \tau^+\tau^-$. In the two upper frames for the Higgs masses, a scan is performed over the same $[\lambda, A_\kappa]$ range as in Fig. 1, which therefore includes the three points P1, P2 and P3. In the lower frames for the Higgs masses and for the branching ratios, a finer scan zooms on the $[\lambda, A_\kappa]$ range which involves only the two points P1 and P2.

A very light $h_1^0$ state (and, thus, with the decay $h_2^0 \to h_1^0 h_1^0$ being the dominant channel) is represented by P4, which can be obtained once one relaxes the universality conditions on the soft SUSY–breaking Higgs mass terms, $m_{H_d} \neq m_{H_u} \neq m_0$. A scenario as in P5, in which all NMSSM Higgs bosons are light, is possible if one allows additionally for $A_\lambda \neq A_0$.

For all benchmark points the numerical value of the pseudoscalar Higgs boson mass $M_{a_1^0}$ is quite sensitive not only to the NMSSM input parameters (notably to the trilinear coupling $A_\kappa$), but also to the employed SM parameters and to the precision with which radiative corrections are computed. Since the numerical values of $M_{a_1^0}$ are phenomenologically much

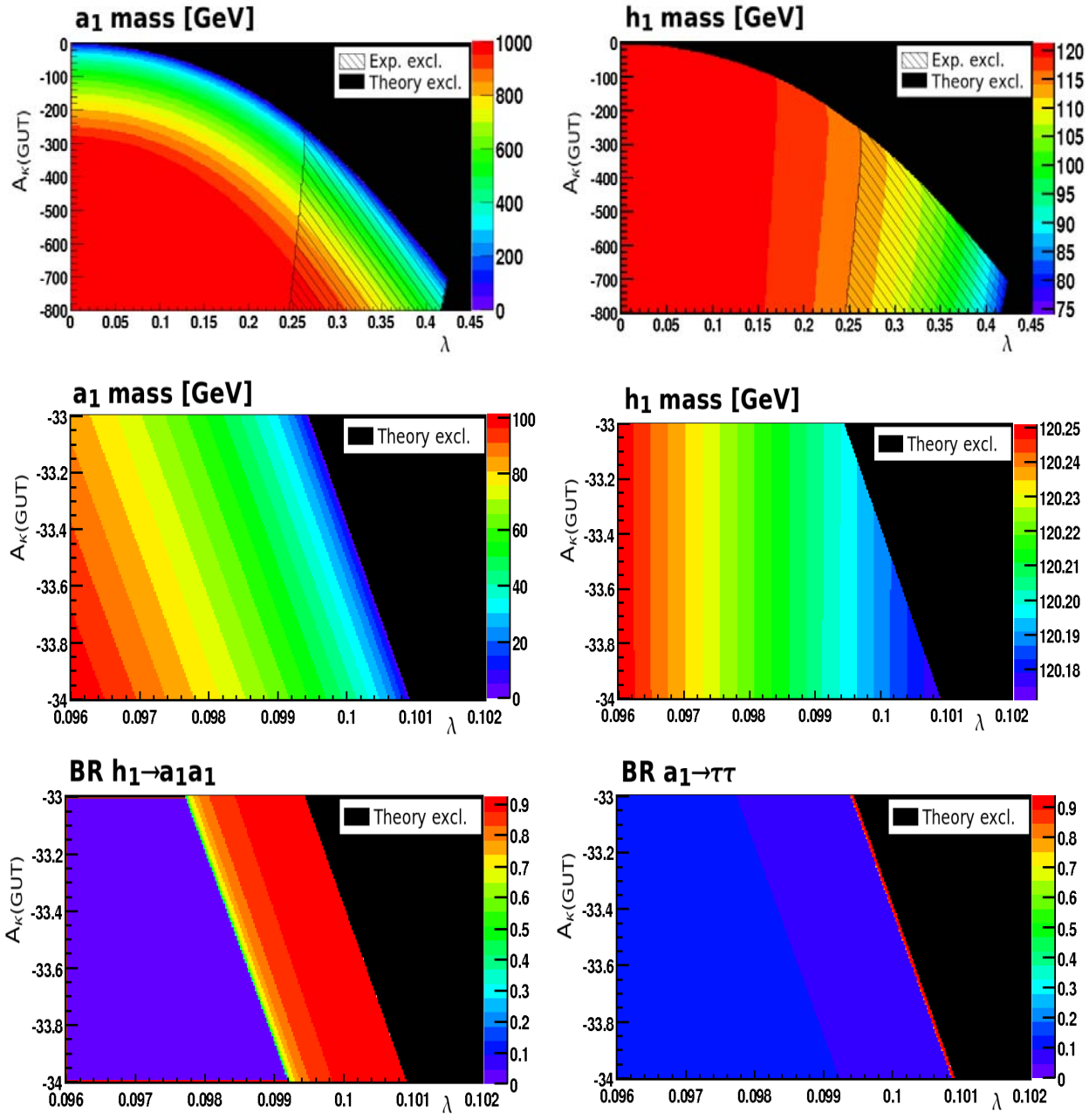


Figure 2: Scans in the $[\lambda, A_\kappa]$ parameter space for the $h_1^0, a_1^0$ masses, and the branching ratios for the decay modes $h_1^0 \to a_1^0 a_1^0$ and $a_1^0 \to \tau^+\tau^-$. The two upper frames include P1 to P3 while the remaining frames include only P1 and P2; other parameters are as in Fig. 1.

more important than, for instance, $A_\kappa$ at $M_{\rm GUT}$, we consider the benchmark points to be defined in terms of $M_{a_1^0}$ rather than in terms of $A_\kappa$ at $M_{\rm GUT}$. Next, we summarize the most relevant phenomenological properties of the benchmark points.

In the first two points P1 and P2, the lightest CP–even Higgs boson has a mass of $M_{h_1^0} \simeq 120$ GeV and is SM–like, as reflected by the corresponding couplings to gauge bosons $R_1$, top quarks $t_1$ and bottom quarks $b_1$, which are almost equal to unity, when normalized to the SM Higgs boson couplings: see Table 1. The lightest CP–odd Higgs boson has masses of 40.5 GeV and 9.09 GeV, which are obtained by choosing $A_\kappa$ at $M_{\rm GUT}$ as $-33.9$ GeV and $-33.4$ GeV, respectively; the remaining parameters of the Higgs sector at $M_{\rm SUSY}$, like $\kappa, A_\lambda, A_\kappa, \mu_{\rm eff}$ and the gaugino mass parameter $M_2$, are given in the second part of Tab. 1.

In both cases P1 and P2, the decay channel $h_1^0 \to a_1^0 a_1^0$ is largely dominating with a branching rate very close to 90%, while the decays $h_1^0 \to b\bar{b}$ and $\tau^+\tau^-$ are suppressed by an order of magnitude as compared to the SM. The most relevant difference between the two scenarios concerns the mass and decays of the lightest pseudoscalar state. In P1 the pseudoscalar $a_1^0$ decays into $b$ quarks and $\tau$ leptons, with branching fractions of $\sim 90\%$ and $\sim 10\%$, respectively. On the other hand, in P2 the pseudoscalar $a_1^0$ with its mass $M_{a_1^0} \simeq 9.09$ GeV decays dominantly into $\tau^+\tau^-$ pairs, with a rate close to 90%.

For point P3, the same inputs of points P1 and P2 are chosen except for the $A_\kappa$ and $\lambda$ parameters, which are now varied as to have a lighter $h_1^0$ state. This again leads to a pseudoscalar Higgs boson which has approximately the same mass as in scenario P2, $M_{a_1^0} \simeq 9.96$ GeV, and which decays almost exclusively into $\tau^+\tau^-$ final states. The difference between P3 and P2 is the lightest CP–even Higgs boson $h_1^0$, which has a mass $M_{h_1^0} \simeq 90$ GeV, lower than in scenarios P1 and P2. In this case, and although $h_1^0$ is still SM–like, exhibiting couplings to gauge bosons, top and bottom quarks that are very close to those of the SM Higgs boson, it decays nevertheless almost exclusively into $a_1^0$ pairs, with a rate close to 100%. Another difference between P2 and P3 is that in the former case the decay mode $h_1^0 \to a_1^0 Z^0$ is kinematically possible but the branching ratio for this new interesting channel that is not listed in the table is rather small, ${\rm BR}(h_1^0 \to a_1^0 Z^0) \sim 3\%$.

Note that in all these first three points, the heaviest neutral Higgs particles $h_2^0, h_3^0$ and $a_2^0$, as well as the charged Higgs states $h^\pm$, all have masses close to or above 1 TeV. The main decay modes are into $b\bar{b}$ and $t\bar{t}$ for the neutral and $tb$ for the charged states, as $\tan\beta$ is not too large and the $t\bar{t}$–Higgs couplings are not very strongly suppressed, while the branching fractions for the neutral Higgs-to-Higgs decays, in particular the channels $h_2^0 \to h_1^0 h_1^0$ and $h_2^0 \to a_1^0 a_1^0$, are very tiny, not exceeding the permille level.

Regarding the properties of the DM candidate, P1, P2 and P3 exhibit a lightest neutralino which is bino–like, and whose mass $m_{\chi_1^0} \simeq 208$ GeV. In all three cases, the correct cosmological density, $\Omega_{\rm CDM} h^2 \simeq 0.1$, is achieved through the co–annihilation with the $\tilde{\tau}_1$ slepton, which has a mass comparable to that of the LSP, $m_{\tilde{\tau}_1} \simeq 213, 213$ and 215 GeV, respectively, for P1, P2 and P3. In each benchmark scenario, the dominant co–annihilation channels are thus $\chi_1^0 \tilde{\tau}_1 \to \gamma\tau$ ($\sim 33\%$) and $\chi_1^0 \tilde{\tau}_1 \to Z^0\tau$ ($\sim 10\%$).

The benchmark point P4 corresponds to a scenario in which the CP–even boson $h_1^0$ is very light, $M_{h_1^0} = 32.3$ GeV, and singlet–like, with a singlet component above 99%. The

Table 1: Input and output parameters for the five benchmark NMSSM points.

| **Point** | P1 | P2 | P3 | P4 | P5 |
|---|---|---|---|---|---|
| **GUT/input parameters** | | | | | |
| $\mathrm{sign}(\mu_{\rm eff})$ | + | + | + | − | + |
| $\tan\beta$ | 10 | 10 | 10 | 2.6 | 6 |
| $m_0$ (GeV) | 174 | 174 | 174 | 775 | 1500 |
| $M_{1/2}$ (GeV) | 500 | 500 | 500 | 760 | 175 |
| $A_0$ | -1500 | -1500 | -1500 | -2300 | -2468 |
| $A_\lambda$ | -1500 | -1500 | -1500 | -2300 | -800 |
| $A_\kappa$ | -33.9 | -33.4 | -628.56 | -1170 | 60 |
| NUHM: $M_{H_d}$ (GeV) | - | - | - | 880 | -311 |
| NUHM: $M_{H_u}$ (GeV) | - | - | - | 2195 | 1910 |
| **Parameters at the SUSY scale** | | | | | |
| $\lambda$ (input parameter) | 0.1 | 0.1 | 0.4 | 0.53 | 0.016 |
| $\kappa$ | 0.11 | 0.11 | 0.31 | 0.12 | -0.0029 |
| $A_\lambda$ (GeV) | -982 | -982 | -629 | -510 | 45.8 |
| $A_\kappa$ (GeV) | -1.63 | -1.14 | -11.4 | 220 | 60.2 |
| $M_2$ (GeV) | 392 | 392 | 393 | 603 | 140 |
| $\mu_{\rm eff}$ (GeV) | 968 | 968 | 936 | -193 | 303 |
| **CP even Higgs bosons** | | | | | |
| $m_{h_1^0}$ (GeV) | 120.2 | 120.2 | 89.9 | 32.3 | 90.7 |
| $R_1$ | 1.00 | 1.00 | 0.998 | 0.034 | -0.314 |
| $t_1$ | 1.00 | 1.00 | 0.999 | 0.082 | -0.305 |
| $b_1$ | 1.018 | 1.018 | 0.975 | -0.291 | -0.644 |
| $\mathrm{BR}(h_1^0 \to bb)$ | 0.072 | 0.056 | $7\times10^{-4}$ | 0.918 | 0.895 |
| $\mathrm{BR}(h_1^0 \to \tau^+\tau^-)$ | 0.008 | 0.006 | $7\times10^{-5}$ | 0.073 | 0.088 |
| $\mathrm{BR}(h_1^0 \to a_1^0 a_1^0)$ | 0.897 | 0.921 | 0.999 | 0.0 | 0.0 |
| $m_{h_2^0}$ (GeV) | 998 | 998 | 964 | 123 | 118 |
| $R_2$ | -0.0018 | -0.0018 | 0.005 | 0.999 | 0.927 |
| $t_2$ | -0.102 | -0.102 | -0.095 | 0.994 | 0.894 |
| $b_2$ | 10.00 | 10.00 | 9.99 | 1.038 | 2.111 |
| $\mathrm{BR}(h_2^0 \to bb)$ | 0.31 | 0.31 | 0.14 | 0.081 | 0.87 |
| $\mathrm{BR}(h_2^0 \to t\bar{t})$ | 0.11 | 0.11 | 0.046 | 0.0 | 0.0 |
| $\mathrm{BR}(h_2^0 \to a_1^0 Z^0)$ | 0.23 | 0.23 | 0.72 | 0.0 | 0.0 |
| $m_{h_3^0}$ (GeV) | 2142 | 2142 | 1434 | 547 | 174 |
| **CP odd Higgs bosons** | | | | | |
| $m_{a_1^0}$ (GeV) | 40.5 | 9.1 | 9.1 | 185 | 99.6 |
| $t_1'$ | 0.0053 | 0.0053 | 0.0142 | 0.0513 | -0.00438 |
| $b_1'$ | 0.529 | 0.528 | 1.425 | 0.347 | -0.158 |
| $\mathrm{BR}(a_1^0 \to bb)$ | 0.91 | 0. | 0. | 0.62 | 0.91 |
| $\mathrm{BR}(a_1^0 \to \tau^+\tau^-)$ | 0.085 | 0.88 | 0.88 | 0.070 | 0.090 |
| $m_{a_2^0}$ (GeV) | 1003 | 1003 | 996 | 546 | 170 |
| **Charged Higgs boson** | | | | | |
| $m_{h^\pm}$ (GeV) | 1005 | 1005 | 987 | 541 | 188 |

Table 2: LSP properties and relic density for the five benchmark NMSSM points.

| **Point** | P1 | P2 | P3 | P4 | P5 |
|---|---|---|---|---|---|
| **Dark matter** | | | | | |
| LSP ($\chi_1^0$) mass (GeV) | 208 | 208 | 208 | 101 | 70.4 |
| $N_{11}$ | 0.999 | 0.999 | 0.999 | -0.039 | 0.977 |
| $N_{12}$ | -0.008 | -0.008 | -0.009 | 0.043 | -0.098 |
| $N_{13}$ | 0.048 | 0.048 | 0.050 | -0.028 | 0.178 |
| $N_{14}$ | -0.015 | -0.015 | -0.016 | 0.405 | -0.068 |
| $N_{15}$ | 0 | 0 | 0.003 | 0.912 | -0.003 |
| $\Omega_{\rm CDM}h^2$ | 0.099 | 0.099 | 0.130 | 0.099 | 0.105 |

lightest scalar Higgs particle predominantly decays into $b\bar{b}$ pairs, with BR($h_1^0 \to b\bar{b}$) = 92%, and to a smaller extent into $\tau$ pairs with BR($h_1^0 \to \tau^+\tau^-$) $\simeq$ 7%. The CP–even $h_2^0$ boson has a mass of $M_{h_2^0} \simeq 123$ GeV and is SM–like, with normalized couplings to $W/Z^0$ and $t/b$ states close to unity. However, since $M_{h_2^0} > 2M_{h_1^0}$, it mostly decays into two $h_1^0$ bosons, with BR($h_2^0 \to h_1^0 h_1^0$) $\simeq$ 88%, and the dominant SM–like $b\bar{b}$ decay mode occurs only at a rate smaller than 10%. The lightest CP–odd particle is not very heavy, $M_{a_1^0} = 185$ GeV, and decays mostly into fermion pairs BR($a_1^0 \to b\bar{b}$) $\sim$ 61% and BR($a_1^0 \to \tau^+\tau^-$) $\sim$ 7%. The other dominant decay is the interesting channel $a_1^0 \to h_1^0 Z^0$ which has a branching ratio of the order of 30%. Finally, the heaviest CP even $h_3^0$ and CP–odd $a_2^0$ states and the charged $h^\pm$ particles have masses in the 500 GeV range and will mostly decay, as $\tan\beta$ is small, into $t\bar{t}/tb$ final states for the neutral/charged states. All these features make the phenomenology of point P4 rather different from that of points P1 to P3 discussed above.

To achieve a correct cosmological relic density, the common sfermion and gaugino mass parameter $m_0$ and $M_{1/2}$ at the GUT scale are set close to 1 TeV. At the SUSY scale, one thus finds a higgsino-singlino-like neutralino LSP, whose mass is $m_{\chi_1^0} \sim 100$ GeV. LSP annihilation essentially occurs via two channels: $\chi_1^0\,\chi_1^0 \to W^+W^-$ (60%) and $\chi_1^0\,\chi_1^0 \to Z^0 h_1^0$ (20%), mediated by $s$–channel $Z^0$ and Higgs boson exchange.

Finally, point P5 is characterized by having all Higgs particles relatively light with masses in the range 90 to 190 GeV. Here, the small value for the coupling $\lambda$ leads to a small value $\kappa \simeq -0.003$. The three CP–even Higgs bosons with masses of 91, 118 and 174 GeV, respectively, share the couplings of the SM Higgs boson to SM gauge bosons with the dominant component being taken by the $h_2^0$ state. The reduced couplings of the state $h_3^0$ for this point, not given in the Table 1, are $R_3 = -0.205$, $t_3 = -0.37$ and $b_3 = 5.7$. The pseudoscalar Higgs bosons have masses $M_{a_1^0} \simeq 100$ GeV and $M_{a_2^0} \simeq 170$ GeV, while the charged Higgs particle is the heaviest one with a mass $M_{h^\pm} \simeq 188$ GeV. Here, all the neutral Higgs-to–Higgs decays are kinematically forbidden. This is also the case of neutral Higgs decays into lighter Higgs states with opposite parity and gauge bosons. The only non–fermionic two–body Higgs decays are thus $h^\pm \to W h_1^0$ and $h_3^0 \to WW$, but as the involved Higgs–gauge boson couplings are small, the branching ratios are tiny.

In this last point P5, the LSP with a mass $m_{\chi_1^0} \sim 70$ GeV, is a bino–like neutralino but has a small non–negligible higgsino component. The correct cosmological relic density $\Omega_{\rm CDM}h^2 \simeq 0.1$ is achieved through the exchange of Higgs bosons in the $s$–channel in the annihilation processes $\chi_1^0\chi_1^0 \to b\bar{b}, \tau^+\tau^-$ which occur at a rate of $\sim 90\%$ and 10%, respectively, i.e. comparable to the Higgs decay branching ratios.

More detailed properties of the benchmark points such as more branching ratios of the Higgs scalars are available on the web site of Ref. [27].

# 4. Implications for the LHC

## 4.1 Dominant production processes

In the cases discussed here, at least one CP–even Higgs particle $h_i^0$ has strong enough couplings to massive gauge bosons or top/bottom quarks, i.e. $R_i, t_i/b_i \sim 1$, to allow for the production at the LHC in one of the main channels which are advocated for the search of the SM Higgs particle [20]:

*i)* gluon–gluon fusion, $gg \to h_i^0$, occurring through a loop of heavy top quarks which couple strongly to the Higgs boson,

*ii)* vector boson fusion, $qq \to qqW^*W^*, qqZ^{0*}Z^{0*} \to qqh_i^0$, which leads to two forward jets and a centrally decaying Higgs boson,

*iii)* the Higgs–strahlung processes, $q\bar{q}' \to Wh_i^0$ and $q\bar{q} \to Z^0h_i^0$, which lead to a Higgs and a massive gauge boson in the final state,

*iv)* associated production with heavy quark pairs $q\bar{q}/gg \to Q\bar{Q}h_i^0$, with $Q = t, b$.

In the scenarios P1 to P3, this CP–even particle is the $h_1^0$ boson which has $R_1 \simeq t_1 \simeq b_1 \simeq 1$, but which decays predominantly into a pair of light pseudoscalar Higgs particles, $h_1^0 \to a_1^0a_1^0$, which subsequently decay into light fermion pairs, $a_1^0 \to b\bar{b}$ and $\tau^+\tau^-$. In scenario P4, this particle is the $h_2^0$ boson which decays most of the time into a pair of $h_1^0$ particles, $h_2^0 \to h_1^0h_1^0$, which again decay into light fermion pairs. In these four cases, the backgrounds for the modes $gg \to h_i^0 \to 4f$ and $qq/gg \to t\bar{t}h_i^0 \to t\bar{t} + 4f$ with $f = b, \tau$, will be extremely large and only the vector boson fusion (owing to the forward jet tagging) and possibly the Higgs–strahlung (due to the leptons coming from the decays of the gauge bosons) can probably be viable at the LHC. Note that in the case of scenario P4, one can try taking advantage of the relatively light $a_1^0$ and the large rate for the interesting and clean decay mode $a_1^0 \to h_1^0Z^0$, which occurs at the level of 2% if the $Z^0$ boson decays into electrons and muons. However, the cross sections for $a_1^0$ production in the $gg \to a_1^0$ and $gg/q\bar{q} \to t\bar{t}a_1^0$ processes, which are the dominant ones for the production of the MSSM CP–odd Higgs boson [20], are very small as the reduced $a_1^0tt$ coupling is very tiny, $t_1' \sim 0.05$. One would have then to rely on associated production of the $a_1^0$ state with a CP–even Higgs boson, such as $q\bar{q} \to Z^{0*} \to a_1^0h_1^0$, but the cross section is not expected to be very large.

In scenario P5, the particle which has couplings to gauge bosons and top quarks that are close to those of the SM Higgs boson is the $h_2^0$ boson which decays into $b\bar{b}$ and $\tau^+\tau^-$ final states with branching ratios close to 90% and 10%, respectively. Here again, the $gg$ fusion and presumably associated production with top quarks cannot be used since the interesting decays such as $h_2^0 \to WW^*, Z^0Z^{0*}$ and $\gamma\gamma$ are suppressed when compared to the SM case (by at least a factor of four as $b_2 \sim 2$). Thus, in this case, only the channels $qq \to qqh_2^0 \to qq\tau^+\tau^-$ and possibly $q\bar{q}' \to Wh_2^0 \to \ell\nu b\bar{b}$ seem feasible. The state $h_1^0$ has still non–negligible couplings to gauge bosons and top quarks which lead to cross sections that are "only" one order of magnitude smaller than in the SM. Since here, only the decays $h_1^0 \to b\bar{b}$ (90%) and $\tau^+\tau^-$ (10%) are again relevant, the only processes which can be used are the vector boson fusion and Higgs–strahlung processes discussed above. Even so, one needs a luminosity 10 times larger to have the same event samples as in the SM. Note that for this point, one can also consider associated CP–even and CP–odd Higgs production, $q\bar{q} \to Z^{0*} \to h_i^0 a_i^0$ but the cross sections are still small. Finally, one should note that for this point, the value of $\tan\beta$ is moderate and thus, the charged Higgs coupling to $tb$ states is the smallest possible, and does not guarantee the detection of the $h^\pm$ bosons.

### 4.2 Summary of available studies

Let us now briefly summarize the few detailed studies (possibly including Monte Carlo simulations) of the LHC potential for the NMSSM Higgs sector that have been performed for scenarios close to the ones discussed here[2].

In scenarios with a very light pseudoscalar Higgs boson, preliminary LHC studies focused on the $qq \to qqWW, qqZ^0Z^0 \to qqh_1^0 \to qqa_1^0a_1^0$ detection mode, i.e. via vector boson fusion (VBF) with forward/backward jet tagging [6]. The hope was that such NMSSM specific scenarios would be visible, particularly if the lightest CP–odd Higgs boson mass allowed for abundant $a_1^0a_1^0 \to b\bar{b}\,\tau^+\tau^-$ decays, with both $\tau$–leptons being detected via their $e, \mu$ leptonic decays. At high luminosity, the VBF signal may be detectable at the LHC as a bump in the tail of a rapidly falling mass distribution of the $2\tau\,2j$ system (without $b$ tagging). However, this procedure relies on the background shape to be accurately predictable. These analyses were based on Monte Carlo (MC) event generation via the SUSY routines of the `HERWIG` code [43] and the toy detector simulation `GETJET`. Further analyses based on the `PYTHIA` generator [44] and the more adequate ATLAS detector simulation `ATLFAST` [45] found that the original selection procedures may need improvement in order to extract a signal.

Also considered was the Higgs–strahlung process with the $q\bar{q}' \to W^* \to W^\pm h_1^0 \to W^\pm a_1^0 a_1^0$ signature, exploiting leptonic decays of gauge bosons with a subleading component from $q\bar{q} \to Z^{0*} \to Z^0 h_1^0 \to Z^0 a_1^0 a_1^0$ and, more marginally, associated production with top quarks, $q\bar{q}, gg \to t\bar{t}h_1^0 \to t\bar{t}a_1^0a_1^0$ [12]. Regardless of the decay modes of the pseudoscalar Higgs bosons, it has been shown in this parton–level analysis, but in which the efficiency to trigger

[2] The prospects for the Tevatron have been discussed in Refs. [11, 13, 15] and seem quite dim.

on the signal is included, that at least the Higgs–strahlung process $q\bar{q} \to W h_1^0$ should be taken into account along with the VBF process to improve the overall signal efficiency. This is particularly true for $h_1^0$ masses below $\sim 90$ GeV where the Higgs–strahlung cross section exceeds that from VBF production. In another parton–level study [16], Higgs–strahlung with $h_1^0 \to a_1^0 a_1^0 \to 4b$ was considered, and it was claimed that with a charged lepton for the $W$ boson and the fully tagged $4b$ final state with Higgs mass reconstruction, the signal could be disentangled from the background. Nevertheless, these results need to be confirmed by MC and detector simulations.

Note that in Ref. [13], the $h_1^0 \to 4\gamma$ final state topology was advocated to be useful for the LHC at very high luminosity if the branching ratio of the decay exceeds the level of $10^{-4}$. However, in general, this decay has a smaller branching ratio and again, a detailed simulation which takes into account the experimental environment is lacking here. The scope of other decays, such as $a_1^0 a_1^0 \to jjjj$ and $jj\,\tau^+\tau^-$ where $j$ represents a light quark jet, is expected to be very much reduced, while the possibilities from $a_1^0 a_1^0 \to 4\tau$ are currently being explored, in both vector boson and Higgs–strahlung production processes.

In scenarios with a very light scalar Higgs boson such as our point P4, constraints from Higgs searches at LEP do not allow for $h_1^0$ masses below about 10 GeV, hence the main decay mode would be $h_1^0 \to b\bar{b}$ while the decay $h_1^0 \to \tau^+\tau^-$ would have a branching ratio of the order of 7–8%. The studies discussed above for very light pseudoscalar Higgs bosons but with the SM–like Higgs boson being the $h_2^0$ state, which then decays into two $h_1^0$ bosons, can therefore be adapted to this case. In particular, the situation for point P4 would be very similar to that of point P1 as the production cross sections, the decay branching ratios and the masses of the involved primary and secondary Higgs bosons are very similar.

Ref. [46] considered a particularly challenging NMSSM scenario, with a Higgs spectrum very similar to that of the MSSM, i.e., nearly degenerate (doublet dominated), heavy charged, scalar and pseudoscalar states and a light scalar Higgs boson at around 120–140 GeV, but including an additional singlet-dominated scalar and a pseudoscalar; such a scenario is somewhat similar to our point P4. Despite of having a reasonably large production cross-sections at the LHC, this light Higgs boson would be difficult to observe since its main hadronic decays cannot be easily disentangled from the QCD backgrounds.

In addition, some studies performed in the CP–violating MSSM, in which the $h_1^0$ boson can also be very light with reduced couplings to gauge bosons, can also be adapted to this context. Note however, that in the case of the CP–violating MSSM, one would also have a light $h^\pm$ boson, while in the NMSSM this state can be very heavy.

Finally, in scenarios in which all NMSSM Higgs bosons are relatively light as in point P5, no detailed analysis has been performed. To our knowledge, the only study that is available is the one performed in Ref. [9] in which the ATLAS and CMS signal significances for the MSSM, assuming a high luminosity of 300 fb$^{-1}$, was rescaled to take into account the reduced couplings of the various Higgs particles to gauge bosons and top quarks. The effect

of almost overlapping resonances, new decay modes or production channels not present in the MSSM analyses of the ATLAS and CMS collaborations have not been considered. In fact, the situation in this scenario looks similar to that of the intense coupling regime of the MSSM [40], in which the three neutral Higgs bosons have masses in the range 100–140 GeV. It was shown in the detailed simulation of Ref. [41] that while it would be very difficult to resolve all Higgs resonances, it would be at least possible to detect one or two Higgs states. However, in the latter case, the value of $\tan\beta$ is assumed to be large, leading to strongly enhanced cross sections in the $gg$ fusion and $b\bar{b}$ Higgs processes, while in the NMSSM one could have relatively moderate $\tan\beta$ values as in P5 and thus, smaller production rates.

### 4.3 ATLAS strategy for NMSSM $h_1^0 \to a_1^0 a_1^0$ searches

At the ATLAS collaboration [47], current efforts to find suitable search channels for special NMSSM phenomenological scenarios are being focused on the vector boson fusion production of a scalar Higgs boson with relatively low mass and subsequent decay via a pair of pseudoscalar Higgs bosons into four $\tau$-leptons, $h_1^0 \to a_1^0 a_1^0 \to 4\tau$. This decay chain is favored in points P2 and P3 proposed here. The main emphasis is presently given to the case where all four $\tau$-leptons decay leptonically.

A typical feature of the vector boson fusion production mode is the so-called tagging jets that are produced from the quarks that are scattered off the heavy vector bosons and merge to give the Higgs boson. These jets typically have high energies and lie in different hemispheres in the forward- and backward regions of the detector. Cutting on this signature is an important means to suppress background processes. Since there is no color flow between the quarks in the vector boson fusion process, jet production in the central detector region is suppressed. In contrast, central emission is favored in QCD interactions which constitute important background processes at the LHC [48]. Experimentally, this can be exploited by vetoing on additional jets in this region.

The decay products of the Higgs boson typically lie in the central detector region. In general, leptons from the same pseudoscalar Higgs boson form pairs that lie close to each other in the detector, the separation being sensitive to the pseudoscalar mass. The invariant mass of the lepton pair has to be lower than the pseudoscalar mass, and is thus much lower than the $Z^0$-mass. For background processes including $Z^0$-bosons, the photon interference therefore needs to be considered. In the experimentally most simple case, all four $\tau$-leptons decay to muons in the process $h_1^0 \to a_1^0 a_1^0 \to 4\tau \to 4\mu + 4\nu_\mu + 4\nu_\tau$. Since muons do not deposit considerable energy in the detector, muons from a very close pair can be also classified as isolated. Decay channels including electrons need more consideration, as their energy is deposited in the calorimeters by electromagnetic showering. The possibility of separating nearby electrons or finding un-isolated muons inside an electromagnetic shower from an electron needs careful study with a full ATLAS detector simulation.

The transverse momentum of the stable leptons in this channel is rather low, since a large

part of the energy is carried away by the eight neutrinos in the final state. Therefore, not in all cases will all four leptons be identified. It might therefore prove favorable to require only three leptons to be found. For triggering, two muons (electrons) with $p_T$ >10 GeV (20 GeV) or one muon (electron) with $p_T$>20 GeV (25 GeV) are needed. It might also be considered to require a minimum transverse momentum for the remaining leptons to avoid having a high number of lepton fakes. Another feature of this channel is the large missing momentum from the eight neutrinos in the final state.

In spite of the eight neutrinos in the final state and the fact that one lepton might remain unrecognized, it is still possible to reconstruct the mass of the scalar Higgs boson with help of the collinear approximation [49] which is also used for mass reconstruction in the VBF, Higgs $\rightarrow \tau\tau$ channel [50]. Since the pseudoscalar bosons and the $\tau$-leptons from their decays obtain a large Lorentz boost due to the large mass and $p_T$ of the Higgs boson, their decay products are emitted roughly in the direction of the original pseudoscalar. Exploiting momentum conservation in the transverse plane yields the 4-momentum vectors of the two pseudoscalars and thus the invariant mass of the scalar Higgs boson. The performance of this algorithm for the $h_1^0 \rightarrow a_1^0 a_1^0 \rightarrow 4\tau \rightarrow 4\mu + 8\nu$ channel is currently under study at ATLAS.

Possible background processes for this channel are $t\bar{t}$ production, vector boson production in association with bottom or top quarks and production of vector boson pairs with additional light jets. Here, the leptons can come from decays of the heavy vector bosons or from decays of the bottom quarks. The tagging jets of the vector boson fusion channel might be faked by untagged $b$-jets or by light jets from other sources in the event. It should be noted that the production of a vector boson pair in association with two light jets contains diagrams that have a structure similar to the vector boson fusion process, with two heavy bosons being scattered off by the incoming quarks and no color flow between the quark lines. Possible methods to separate these background processes from the signal and their performance are currently studied by the ATLAS-collaboration.

### 4.4 Prospects for the CMS experiment

The final state topology $h_1^0 \rightarrow a_1^0 a_1^0 \rightarrow \tau^+\tau^-\tau^+\tau^-$ where the $\approx$ 100 GeV $h_1^0$ state is produced in the VBF process and the pseudoscalar $a_1^0$ boson has a mass $2m_\tau < M_{a_1^0} < 2m_b$ (so that the $a_1^0 \rightarrow \tau^+\tau^-$ decay mode is dominant) is currently under investigation by the CMS collaboration for the $\mu^\pm\mu^\pm\tau_{\rm jet}^\mp\tau_{\rm jet}^\mp$ final state containing two same sign muons and two $\tau$ jets. The $\tau$ leptons from the decays of the light $a_1^0$ state are approximately collinear and the non-isolated, di–muon high level trigger is needed to select the signal events. The standard CMS di-muon trigger with the relaxed isolation has the di-muon threshold of 10 GeV on both muons for a luminosity $\mathcal{L} = 2 \times 10^{33}$ cm$^{-2}$s$^{-1}$ [52] and, since the muons from the signal events are very soft, the lower thresholds are needed. For instance, with a 7 GeV threshold the efficiency is increased approximately by a factor of two, but the QCD background rate

is also increased by the same factor [53] which is not acceptable. In order to cope with the rate, the same-sign relaxed di-muon trigger was recently introduced [54]. A PYTHIA simulation shows that the rate of di-muons from $b\bar{b}$ production is reduced by a factor of four when asking for the two same sign muons to have a threshold of 5 GeV. The off-line selection strategy requires the presence of the two same sign, non-isolated muons with one track in the cone around each muon direction, thus selecting the one prong $\tau$ decays.

For a point with masses $M_{h_1^0} \sim 100$ GeV and $M_{a_1^0} \sim 5$ GeV, one applies the following basic event selection cuts at the generation level: *i*) two same sign muons with $p_T$ >7 GeV and $|\eta|$ <2.1 with one track of $p_T$ >1 GeV in a cone 0.3 around each muon; *ii*) opposite charge for the muon and the track; *iii*) two $\tau$ jets with $p_T$ >10 GeV and $|\eta|$ <2.1; *iv*) two jets with $p_T$ >30 GeV and $|\eta|$ <4.5. After these cuts, and using the SM VBF Higgs production cross section which is approximately 5.4 pb for the considered $h_1^0$ mass, the cross section of the signal after all selections is around 2 fb, leading to $\approx 60$ events at a luminosity of 30 fb$^{-1}$. The dominant backgrounds with two non isolated muons from the $b\bar{b}$ and $t\bar{t}$ production processes are under evaluation.

For heavier $a_1^0$ bosons as in scenarios P2 and P3 where $M_{a_1^0} \sim 10$ GeV, the "non isolation" requirement should be relaxed since two $\tau$ leptons from the $a_1^0 \to \tau\tau$ decay are more separated and one should accept zero or one track in the cone (note that the relaxed di-muon trigger accepts both isolated and non isolated muons). One needs, however, to consider the backgrounds with isolated muons from $W$ and $Z^0$ decays, in addition to $b\bar{b}$ and $t\bar{t}$.

The $h_1^0 \to a_1^0 a_1^0 \to \tau^+\tau^-\tau^+\tau^-$ decay with $h_1^0$ produced in Higgs–strahlung with leptonic decays of the $W$ bosons, which can give a very clean and almost background free signal, is also being considered by the CMS collaboration. The leptons coming from $W$ decays allow to trigger on the events and the CMS single isolated lepton trigger can be used [53]. The signal is unique as one has two collinear $\tau$ leptons due to the large boost of $a_1^0$ bosons and, potentially, the most interesting final state is when one of the $\tau$s decays hadronically and the other decays into muons.

As for the selection criteria and the muon and $\tau$ identification, for each $\tau$-jet candidate there must be a muon in the $\tau$-jet cone. The $\tau$ jet and the muon are required to be oppositely charged and the events with two identified $\tau$ jets with $E_T > 10$ GeV and two muons with $p_T > 7$ GeV are selected. Unlike in the VBF case, the muons are not required to have the same sign. Finally, the events with extra jets on top of two $\tau$ jets are rejected. A preliminary, full detector simulation and reconstruction analysis of the signal events in a scenario with $M_{h_1^0} \sim 100$ GeV and $M_{a_1^0} \sim 5$ GeV shows that after all selection cuts, one expects $\approx 10$ events for 30 fb$^{-1}$ data if the SM cross section of $\sim 2.6$ pb and a branching ratio BR($h_1^0 \to a_1^0 a_1^0$) $\simeq 0.9$ are assumed. The potential backgrounds are $t\bar{t}, tW$, QCD multijet, $W$+jets and $b\bar{b}$ events. Preliminary tests with full detector simulation show that the requirement of two $\tau$ jets, both having an oppositely charged muon in the jet cone, as well as jet veto suppresses the backgrounds very efficiently.

## 5. Conclusions

The NMSSM is a very interesting supersymmetric extension of the SM, as it solves the notorious $\mu$ problem of the MSSM and it has less fine tuning. It also leads to an interesting collider phenomenology in some cases, in particular in the Higgs sector, which is extended to contain an additional CP–even and CP–odd state as compared to the MSSM. Hence, the searches for the NMSSM Higgs bosons will be rather challenging at the LHC in scenarios in which some neutral Higgs particles are very light, opening the possibility of dominant Higgs to Higgs decays, or when all Higgs bosons are relatively light but have reduced couplings to the electroweak gauge bosons and to the top quarks, compared to the SM Higgs case. These scenarios require much more detailed phenomenological studies and experimental simulations to make sure that at least one Higgs particle of the NMSSM will be observed at the LHC.

In this note, we have proposed benchmark points in which these difficult scenarios are realized in a semi–unified NMSSM which involves a rather limited number of input parameters at the grand unification scale and which fullfils all present collider and cosmological constraints. In three of the five benchmark scenarios introduced here, the lightest CP–even Higgs boson decays mainly in two very light pseudoscalar Higgs states which subsequently decay into two $b$ quarks or $\tau$ leptons, leading to four fermion final states; in a fourth scenario, the next–to–lightest CP–even Higgs boson has a mass of $\sim 120$ GeV and couplings to fermions and gauge bosons that are SM–like but it decays into pairs of the lightest Higgs state, which then decays into a $b\bar{b}$ pair; in a last scenario, all neutral and charged Higgs particles are light (with masses less than $\sim 180$ GeV) and have weaker couplings to $W/Z^0$ bosons than the SM Higgs particle. We have analysed the Higgs and supersymmetric particle spectra of these benchmark scenarios, discussed the various decay and production rates as well as other phenomenological implications and attempted to set the basis for the search strategies to be followed by the ATLAS and CMS collaborations in order to observe at least one of the neutral Higgs states in these scenarios.

### Addendum

After the completion of this paper, discussions of various possibilities of the observation of the cascade decay $h_1^0 \to a_1^0 a_1^0 \to ...$ at hadron colliders appeared in Refs. [56].


### Acknowledgments

AD is grateful to the Leverhulme Trust (London, UK) for partial financial support in the form a Visiting Professorship to the NExT Institute (Southampton & RAL, UK) and to the Alexander von–Humbold Foundation (Bonn, Germany). SM acknowledges financial support from The Royal Society (London, UK). We acknowledge support from the FP7 RTN MRTN-CT-2006-035505 (HEPTOOLS), the French ANR project PHYS@COL&COS and the Indo–French Center IFCPAR for the project number 3004-2. We also thank the organisers of the 2007 Les Houches workshop on 'Physics at TeV Colliders' for the nice working framework.

# References


[1] P. Fayet, Nucl. Phys. B **90** (1975) 104; Phys. Lett. B **64** (1976) 159; Phys. Lett. B **69** (1977) 489 and Phys. Lett. B **84** (1979) 416; H.P. Nilles, M. Srednicki and D. Wyler, Phys. Lett. B **120** (1983) 346; J.M. Frere, D.R. Jones and S. Raby, Nucl. Phys. B **222** (1983) 11; J.P. Derendinger and C.A. Savoy, Nucl. Phys. B **237** (1984) 307; A.I. Veselov, M.I. Vysotsky and K.A. Ter-Martirosian, Sov. Phys. JETP **63** (1986) 489; J.R. Ellis, J.F. Gunion, H.E. Haber, L. Roszkowski and F. Zwirner, Phys. Rev. D **39** (1989) 844; M. Drees, Int. J. Mod. Phys. A **4** (1989) 3635.

[2] U. Ellwanger, M. Rausch de Traubenberg and C.A. Savoy, Phys. Lett. B **315** (1993) 331; Z. Phys. C **67** (1995) 665 and Nucl. Phys. B **492** (1997) 307.

[3] U. Ellwanger, Phys. Lett. B **303** (1993) 271; P. Pandita, Z. Phys. C **59** (1993) 575; T. Elliott, S.F. King and P.L. White, Phys. Rev. D **49** (1994) 2435; S.F. King and P.L. White, Phys. Rev. D **52** (1995) 4183; F. Franke and H. Fraas, Int. J. Mod. Phys. A **12** (1997) 479; D. Miller, R. Nevzorov and P.M. Zerwas, Nucl. Phys. B **681** (2004) 3.

[4] J.E. Kim and H.P. Nilles, Phys. Lett. B **138** (1984) 150.

[5] B.A. Dobrescu, G. Landsberg and K.T. Matchev, Phys. Rev. D **63** (2001) 075003; B.A. Dobrescu and K.T. Matchev, JHEP **0009** (2000) 031.

[6] U. Ellwanger, J.F. Gunion, C. Hugonie and S. Moretti, arXiv:hep-ph/0305109 and arXiv:hep-ph/0401228; K.A. Assamagan *et al.* [Higgs Working Group Collaboration], "The Higgs working group: Summary report 2003," arXiv:hep-ph/0406152; G. Weiglein *et al.* [LHC/LC Study Group], Phys. Rept. **426** (2006) 47.

[7] U. Ellwanger, J.F. Gunion and C. Hugonie, JHEP **0502** (2005) 066.

[8] R. Dermisek and J.F. Gunion, Phys. Rev. Lett. **95** (2005) 041801 and arXiv:0705.4387 [hep-ph].

[9] U. Ellwanger, J.F. Gunion and C. Hugonie, JHEP **0507** (2005) 041.

[10] R. Dermisek and J.F. Gunion, Phys. Rev. D **73** (2006) 111701 and Phys. Rev. D **75** (2007) 075019; S. Chang, P.J. Fox and N. Weiner, JHEP **0608** (2006) 068.

[11] P.W. Graham, A. Pierce and J.G. Wacker, arXiv:hep-ph/0605162.

[12] S. Moretti, S. Munir and P. Poulose, Phys. Lett. B **644** (2007) 241; C. Hugonie and S. Moretti, arXiv:hep-ph/0110241.

[13] S. Chang, P.J. Fox and N. Weiner, Phys. Rev. Lett. **98** (2007) 111802.

[14] R. Dermisek and J.F. Gunion, Phys. Rev. D **75** (2007) 075019.

[15] T. Stelzer, S. Wiesenfeldt and S. Willenbrock, Phys. Rev. D **75** (2007) 077701; U. Aglietti *et al.*, "Tevatron-for-LHC report: Higgs," arXiv:hep-ph/0612172.

[16] K. Cheung, J. Song and Q. S. Yan, Phys. Rev. Lett. **99** (2007) 031801.

[17] G. Belanger, F. Boudjema, C. Hugonie, A. Pukhov and A. Semenov, JCAP **0509** (2005) 001; J.F. Gunion, D. Hooper and B. McElrath, Phys. Rev. D **73** (2006) 015011; D.G. Cerdeno, E. Gabrielli, D.E. Lopez-Fogliani, C. Munoz and A.M. Teixeira, JCAP **0706** (2007) 008; V. Barger, P. Langacker, I. Lewis, M. McCaskey, G. Shaughnessy and B. Yencho, Phys. Rev. D **75** (2007) 115002; C. Hugonie, G. Belanger and A. Pukhov, arXiv:0707.0628 [hep-ph].

[18] M. Bastero-Gil, C. Hugonie, S.F. King, D.P. Roy and S. Vempati, Phys. Lett. B **489** (2000) 359.

[19] P.C. Schuster and N. Toro, arXiv:hep-ph/0512189.

[20] For reviews of the SM and MSSM Higgs sectors, see A. Djouadi, arXiv:hep-ph/0503172 and arXiv:hep-ph/0503173, Phys. Repts. in press.

[21] J. Dai, J.F. Gunion, R. Vega, Phys. Lett. B **315** (1993) 355 and Phys. Lett. B **345** (1995) 29; D. Denegri *et al.*, arXiv:hep-ph/0112045; M. Schumacher, arXiv:hep-ph/0410112.

[22] J.F. Gunion, H.E. Haber and T. Moroi, arXiv:hep-ph/9610337; U. Ellwanger, J.F. Gunion and C. Hugonie, arXiv:hep-ph/0111179; G. Azuelos *et al.*, arXiv:hep-ph/0204031.

[23] C. Hugonie and S. Moretti, arXiv:hep-ph/0110241; S. Moretti and S. Munir, Eur. Phys. J. C **47** (2006) 791.

[24] See for instance: B.C. Allanach *et al.*, arXiv:hep-ph/0202233; J.A. Aguilar-Saavedra *et al.*, Eur. Phys. J. C **46** (2006) 43.

[25] See for instance: M. Carena, S. Heinemeyer, C. E. M. Wagner and G. Weiglein, arXiv:hep-ph/9912223; S. Heinemeyer, Int. J. Mod. Phys A **21** (2006) 2659; The LEP Collaboration (ALEPH, DELPHI, L3 and OPAL), Phys. Lett. B **565** (2003) 61.

[26] U. Ellwanger and C. Hugonie, Comput. Phys. Commun. **175** (2006) 290.

[27] U. Ellwanger and C. Hugonie, Comput. Phys. Commun. **177** (2007) 399
(see also http://www.th.u-psud.fr/NMHDECAY/nmssmtools.html).

[28] M. Cvetic, D.A. Demir, J.R. Espinosa, L.L. Everett and P. Langacker, Phys. Rev. D **56** (1997) 2861 [Erratum-ibid. D **58** (1998) 119905]; P. Langacker and J. Wang, Phys. Rev. D **58** (1998) 115010; C. Panagiotakopoulos and K. Tamvakis, Phys. Lett. B **446** (1999) 224 and Phys. Lett. B **469** (1999) 145; C. Panagiotakopoulos and A. Pilaftsis, Phys. Rev. D **63** (2001) 055003; A. Dedes, C. Hugonie, S. Moretti and K. Tamvakis, Phys. Rev. D **63** (2001) 055009; A. Menon, D. E. Morrissey and C. E. M. Wagner, Phys. Rev. D **70** (2004) 035005; T. Han, P. Langacker and B. McElrath, Phys. Rev. D **70** (2004) 115006; D.A. Demir, G.L. Kane and T.T. Wang, Phys. Rev. D **72** (2005) 015012; S.F. King, S. Moretti and R. Nevzorov, Phys. Lett. B **634** (2006) 278 and Phys. Rev. D **73** (2006) 035009; V. Barger, P. Langacker, H.S. Lee and G. Shaughnessy, Phys. Rev. D **73** (2006) 115010.

[29] M. Matsuda and M. Tanimoto, Phys. Rev. D **52** (1995) 3100; N. Haba, Prog. Theor. Phys. **97** (1997) 301; S.W. Ham, S.K. Oh and D. Son, Phys. Rev. D **65** (2002) 075004; M. Boz, Mod. Phys. Lett. A **21** (2006) 243; S.W. Ham, S.H. Kim, S.K. OH and D. Son, arXiv:0708.2755 [hep-ph].

[30] U. Ellwanger and C. Hugonie, Eur. Phys. J. C **5** (1998) 723 and Eur. Phys. J. C **13** (2000) 681; V. Barger, P. Langacker and G. Shaughnessy, Phys. Lett. B **644** (2007) 361 and Phys. Rev. D **75** (2007) 055013.

[31] J.A. Casas, J.R. Espinosa and I. Navarro, Nucl. Phys. B **620** (2002) 195; A. Birkedal, Z. Chacko and Y. Nomura, Phys. Rev. D **71** (2005) 015006.

[32] For recent analyses, see for instance: J.R. Ellis, S. Heinemeyer, K.A. Olive and G. Weiglein, JHEP **0605** (2006) 005, and Phys. Lett. B **653** (2007) 292.

[33] A. Djouadi, J. Kalinowski, P. Ohmann and P.M. Zerwas, Z. Phys. C **74** (1997) 93.

[34] A. Djouadi, M. Spira and P.M. Zerwas, Phys. Lett. B **264** (1991) 440 and Z. Phys. C **70** (1996) 427; M. Spira *et al.*, Nucl. Phys. B **453** (1995) 17; A. Djouadi, J. Kalinowski and M. Spira, Comput. Phys. Commun. **108** (1998) 56.

[35] J. Gunion and H. Haber, Nucl. Phys. B **272** (1986) 1; P. Kalyniak, R. Bates and J. Ng, Phys. Rev. D **33** (1986) 755 and Phys. Rev. D **34** (1986) 172; J. Gunion, G. Gamberini and S. Novaes, Phys. Rev. D **38** (1988) 3481; A. Djouadi, V. Driesen, W. Hollik and J. Illana, Eur. Phys. J. C **1** (1998) 149; A. Djouadi, Phys. Lett. B **435** (1998) 101.

[36] S. Schael *et al.* [ALEPH, DELPHI, L3 and OPAL Collaborations], Eur. Phys. J. C **47** (2006) 547.

[37] G. Hiller, Phys. Rev. D **70** (2004) 034018; F. Domingo and U. Ellwanger, JHEP **0712** (2007) 090.

[38] G. Belanger, F. Boudjema, A. Pukhov and A. Semenov, Comput. Phys. Commun. **149** (2002) 103, and Comput. Phys. Commun. **174** (2006) 577.

[39] J. Hamann, S. Hannestad, M. Sloth and Y. Wong, Phys. Rev. D **75** (2007) 023522.

[40] E. Boos *et al.*, Phys. Rev. D **66** (2002) 055004; E. Boos *et al.*, Phys. Lett. B **622** (2005) 311; A. Djouadi and Y. Mambrini, JHEP **0612** (2006) 001.

[41] E. Boos, A. Djouadi and A. Nikitenko, Phys. Lett. B **578** (2004) 384.

[42] U. Ellwanger and C. Hugonie, Mod. Phys. Lett. A **22** (2007) 1581.

[43] S. Moretti, K. Odagiri, P. Richardson, M. H. Seymour and B. R. Webber, JHEP **0204** (2002) 028; G. Corcella *et al.*, JHEP **0101** (2001) 010.

[44] T. Sjostrand, L. Lonnblad and S. Mrenna, arXiv:hep-ph/0108264.

[45] S. Baffioni, talk presented at "GdR Supersymétrie 2004", 5-7 July 2004, Clermont-Ferrand, France; S. Baffioni and D. Zerwas, private communication.

[46] D.J. Miller and S. Moretti, arXiv:hep-ph/0403137.

[47] ATLAS collaboration, CERN-LHCC-99-014/CERN-LHCC-99-015.

[48] V. D. Barger, R. J. N. Phillips and D. Zeppenfeld, Phys. Lett. B **346** (1995) 106; D. L. Rainwater and D. Zeppenfeld, JHEP **9712** (1997) 005.

[49] R. K. Ellis, I. Hinchliffe, M. Soldate and J. van der Bij, Nucl. Phys. B **297** (1988) 221.

[50] S. Asai *et al.*, Eur. Phys. J. C **32S2** (2004) 19.

[51] I. Rottländer, M. Schumacher *et al.*, to appear.

[52] CMS Physics TDR, Volume II, CERN/LHCC 2006-021, CMS TDR 8.2, 26 June 2006.

[53] The CMS Trigger and Data Acqusition project, Volume II, CERN/LHCC 2002-26, CMS TDR 6.2, 15 Dec. 2002.

[54] The CMS High Level Trigger, CERN/LHCC 2007-021, LHCC-G-134, 29 June 2007.

[55] S. Lehti, A. Nikitenko *et al.*, to appear.

[56] M. Carena, T. Han, G. Y. Huang and C. E. M. Wagner, arXiv:0712.2466 [hep-ph]; J.R. Forshaw, J.F. Gunion, L. Hodgkinson, A. Papaefstathiou and A.D. Pilkington, arXiv:0712.3510 [hep-ph]; R. Barbieri, L.J. Hall, A. Papaioannou, D. Pappadopulo, V. Rychkov arXiv:0712.2903 [hep-ph].